International Journal of Mechanical, Industrial and Aerospace Sciences
ISSN: 2517-9950
Vol:11, No:3, 2017

# Effect of Inclusions on the Shape and Size of Crack Tip Plastic Zones by Element Free Galerkin Method

A. Jameel, G. A. Harmain, Y. Anand, J. H. Masoodi, F. A. Najar

***Abstract*—**The present study investigates the effect of inclusions on the shape and size of crack tip plastic zones in engineering materials subjected to static loads by employing the element free Galerkin method (EFGM). The modeling of the discontinuities produced by cracks and inclusions becomes independent of the grid chosen for analysis. The standard displacement approximation is modified by adding additional enrichment functions, which introduce the effects of different discontinuities into the formulation. The level set method has been used to represent different discontinuities present in the domain. The effect of inclusions on the extent of crack tip plastic zones is investigated by solving some numerical problems by the EFGM.

***Keywords*—**EFGM, stress intensity factors, crack tip plastic zones, inclusions.

## I. Introduction

DIFFERENT types of inclusions are present in engineering components, which have a considerable effect on the crack tip plastic zones developed ahead of the crack tip. Therefore, it is very important to estimate the size and shape of crack tip plastic zones in the presence of inclusions. Several numerical methods have been used to model the discontinuities produced by cracks, inclusions, holes and contact surfaces, such as the finite element method [1], the extended finite element method (XFEM) [2], the boundary element method [3], [4] and mesh free methods [5]-[7]. The conventional finite element method has evolved as the most dominant numerical tool in computational mechanics, but it requires conformal meshing for modeling different discontinuities, which is very difficult and computationally more demanding.

The EFGM handles different types of discontinuities more efficiently than the finite element method because of its meshless approach [8], [9]. The moving least square (MLS) shape functions are used for approximating the displacement field in EFGM. The boundary conditions cannot be applied directly in EFGM because the MLS shape functions do not satisfy the Kronecker delta property. In recent times, several numerical techniques have been developed for imposing the boundary conditions in EFGM, such as the Lagrange multiplier method [10], the penalty method [11] and coupled FE-EFG method [12]. Until now, EFGM has been successfully applied to solve the problems of fracture mechanics [13], [14], frictional contact analysis [15], metal forming analysis [16], large deformation analysis [17], and three-dimensional crack growth [18], [19].

The present approach employs the EFGM for investigating the effect of inclusions on the shape and size of plastic zones developed ahead of the crack tips. The stress intensity factors have been obtained by employing the domain based interaction integral approach [19]. The level set method is used to keep track of different discontinuities present in the domain. Finally, several numerical studies are performed on an edge cracked plate containing inclusions of different sizes and at different positions.

Azher Jameel and Yatheshth Anand are with the Department of Mechanical Engineering, Shri Mata Vaishno Devi University, Katra, JK, India-182320 (phone: +918715028970, e-mail: jameelazher@gmail.com).

G. A. Harmain, Junaid H. Masoodi and Farooq A. Najar are with the Department of Mechanical Engineering, National Institute of Technology, Srinagar, JK, India-190006 (e-mail: gharmain@nitsri.net).

## II. Mathematical Formulations

### A. Modeling of Cracks by EFGM

The equilibrium equation of a loaded body can be written as $\nabla.\sigma + b = 0$, where σ is the stress tensor and b represents the body force vector. For linear elastic materials, we have $\sigma = D\varepsilon$, where D represents the elastic constitutive matrix and ε is the strain tensor. The equilibrium equation can be written in the integral form as:

$$\int_{\Omega} \boldsymbol{\varepsilon}^T \boldsymbol{\sigma}\, d\Omega - \int_{\Omega} \boldsymbol{u}^T \boldsymbol{b}\, d\Omega - \int_{\Gamma_t} \boldsymbol{u}^T \boldsymbol{t}\, d\Gamma_t = 0 \quad (1)$$

where u represents the displacement field and t denotes the traction vector. The enriched displacement based approximation for modeling cracks can be written as:

$$u^h(x) = \sum_{i=1}^{n} \Psi_i(x) u_i + \sum_{i=1}^{n_s} \Psi_i(x)\,[H(x) - H(x_i)]a_i + \sum_{i=1}^{n_T} \Psi_i(x) \sum_{\alpha=1}^{4} [\beta_\alpha(x) - \beta_\alpha(x_i)] b_i^\alpha \quad (2)$$

where $u^h$represents the displacement approximation, $u_i$ are the standard degrees of freedom, $a_i$ and $b_i^\alpha$ are the enriched degrees of freedom corresponding to split and tip nodes respectively and $n, n_s, n_T$ represent the standard, split and tip nodes respectively. $\Psi_i$ are the MLS shape functions used in EFGM. The Heaviside jump function $'H(x)'$ produces the discontinuity in the displacement field across the crack surface. The crack tip enrichment functions $\beta_\alpha(x)$ can be written for linear elastic materials as [19]:

$$\beta_\alpha(x) = [\sqrt{r}cos\tfrac{\theta}{2}, \sqrt{r}sin\tfrac{\theta}{2}, \sqrt{r}cos\tfrac{\theta}{2}sin\theta, \sqrt{r}sin\tfrac{\theta}{2}sin\theta] \quad (3)$$

The substitution of the displacement approximation (2) into the equilibrium equation (1) yields the final numerical model $[\mathbf{K^e}]\{\mathbf{d}^e\} = \{\mathbf{f}^e\}$, where $\mathbf{K}^e$and $\mathbf{f}^e$ are the global stiffness matrix and the force vector, respectively, and $\{\mathbf{d^e}\} = \{\mathbf{u\ a\ b_1\ b_2\ b_3\ b_4}\}^T$. We have:

$$[\mathrm{K}^e] = \begin{bmatrix} \mathrm{K}^{uu} & \mathrm{K}^{ua} & \mathrm{K}^{ub} \\ \mathrm{K}^{au} & \mathrm{K}^{aa} & \mathrm{K}^{ab} \\ \mathrm{K}^{bu} & \mathrm{K}^{ba} & \mathrm{K}^{bb} \end{bmatrix}; \{\mathrm{f}^e\} = \{\mathrm{f}^u\ \mathrm{f}^a\ \mathrm{f}^{b1}\ \mathrm{f}^{b2}\ \mathrm{f}^{b3}\ \mathrm{f}^{b4}\}^T \quad (4)$$

such that

$$\mathbf{K}^{rs} = \int_{\Omega^e} (\mathbf{B}^r)^T \mathbf{D} \mathbf{B}^s d\Omega, r, s = u, a, b \quad (5)$$

$$\mathbf{f}^u = \int_{\Omega^e} \mathbf{\Psi}^T \mathbf{b}\, d\Omega + \int_{\Gamma^e} \mathbf{\Psi}^T \mathbf{t}\, d\Gamma \quad (6)$$

$$\mathbf{f}^a = \int_{\Omega^e} \mathbf{\Psi}^T \big(H(x) - H(x_i)\big)\mathbf{b}\, d\Omega + \int_{\Gamma^e} \mathbf{\Psi}^T (H(x) - H(x_i))\mathbf{t}\, d\Gamma \quad (7)$$

$$\mathbf{f}^{b\alpha} = \int_{\Omega^e} \mathbf{\Psi}^T \big(\beta_\alpha(x) - \beta_\alpha(x_i)\big)\mathbf{b}\, d\Omega + \int_{\Gamma^e} \mathbf{\Psi}^T (\beta_\alpha(x) - \beta_\alpha(x_i))\mathbf{t}\, d\Gamma\ (\alpha = 1,2,3,4) \quad (8)$$

$$\mathbf{B}^u = \begin{bmatrix} \Psi_{i,x} & 0 \\ 0 & \Psi_{i,y} \\ \Psi_{i,y} & \Psi_{i,x} \end{bmatrix} \quad (9)$$

$$\mathbf{B}^a = \begin{bmatrix} (\Psi_i(H(x) - H(x_i)))_{,x} & 0 \\ 0 & (\Psi_i(H(x) - H(x_i)))_{,y} \\ (\Psi_i(H(x) - H(x_i)))_{,y} & (\Psi_i(H(x) - H(x_i)))_{,x} \end{bmatrix} \quad (10)$$

$$\mathbf{B}^{b\alpha} = \begin{bmatrix} (\Psi_i(\beta_\alpha(x) - \beta_\alpha(x_i)))_{,x} & 0 \\ 0 & (\Psi_i(\beta_\alpha(x) - \beta_\alpha(x_i)))_{,y} \\ (\Psi_i(\beta_\alpha(x) - \beta_\alpha(x_i)))_{,y} & (\Psi_i(\beta_\alpha(x) - \beta_\alpha(x_i)))_{,x} \end{bmatrix} \quad (11)$$

*B. Modeling of Inclusions by EFGM*

The displacement field is continuous across the material interface of the inclusion, whereas a discontinuity is created in the strain fields. The enrichment function F(x) used for modeling the discontinuities produced by inclusions can be written as [19]:

$$F(x) = \sum_i |\phi_i| \Psi_i(x) - \left|\sum_i \phi_i \Psi_i(x)\right| \quad (12)$$

where $'\phi'$represents the level sets. The displacement approximation for modeling inclusions can be written as:

$$u^h(x) = \sum_{i=1}^{n} \Psi_i(x) u_i + \sum_{i=1}^{n_s} \Psi_i(x)\,[F(x) - F(x_i)]a_i \quad (13)$$

Substitution of the displacement approximation (13) into the equilibrium equation yields the final system of discrete equations as $[\mathbf{K}^e]\{\mathbf{d}^e\} = \{\mathbf{f}^e\}$, where

$$[\mathbf{K}^e] = \begin{bmatrix} \mathbf{K}^{uu} & \mathbf{K}^{ua} \\ \mathbf{K}^{au} & \mathbf{K}^{aa} \end{bmatrix}; \{\mathbf{f}^e\} = \{\mathbf{f}^u\ \mathbf{f}^a\}^T; \{\mathbf{d}^e\} = \{\mathbf{u\ a}\}^T \quad (14)$$

such that

$$\mathbf{K}^{rs} = \int_{\Omega^e} (\mathbf{B}^r)^T \mathbf{D} \mathbf{B}^s d\Omega\ ; r, s = u, a \quad (15)$$

$$\mathbf{f}^u = \int_{\Omega^e} \mathbf{\Psi}^T \mathbf{b}\, d\Omega + \int_{\Gamma^e} \mathbf{\Psi}^T \mathbf{t}\, d\Gamma \quad (16)$$

$$\mathbf{f}^a = \int_{\Omega^e} \mathbf{\Psi}^T \big(F(x) - F(x_i)\big)\mathbf{b}\, d\Omega + \int_{\Gamma^e} \mathbf{\Psi}^T (F(x) - F(x_i))\mathbf{t}\, d\Gamma \quad (17)$$

$$\mathbf{B}^u = \begin{bmatrix} \Psi_{i,x} & 0 \\ 0 & \Psi_{i,y} \\ \Psi_{i,y} & \Psi_{i,x} \end{bmatrix} \quad (18)$$

$$\mathbf{B}^a = \begin{bmatrix} (\Psi_i(F(x) - F(x_i)))_{,x} & 0 \\ 0 & (\Psi_i(F(x) - F(x_i)))_{,y} \\ (\Psi_i(F(x) - F(x_i)))_{,y} & (\Psi_i(F(x) - F(x_i)))_{,x} \end{bmatrix} \quad (19)$$

*C. Imposition of Boundary Conditions in EFGM*

The Lagrangian multiplier technique has been used for imposing the essential boundary conditions in EFGM. With the help of the Lagrangian multiplier technique, the equilibrium equation of a loaded body can be written as:

$$\int_\Omega\ \boldsymbol{\varepsilon}^T \boldsymbol{\sigma}\, \mathrm{d}\Omega - \int_\Omega\ \mathbf{u}^T \mathbf{b}\, \mathrm{d}\Omega - \int_{\Gamma_t}\ \mathbf{u}^T \mathbf{t}\, \mathrm{d}\Gamma_t + \int_{\Gamma_u}\ \boldsymbol{\lambda}^T (\mathbf{u} - \bar{\mathbf{u}}) \mathbf{d}\Gamma_u = 0 \quad (20)$$

where $\bar{\mathbf{u}}$ represents the prescribed displacement at the displacement boundary $\Gamma_u$ and $\boldsymbol{\lambda}$ denotes the Lagrangian multipliers. With these modifications, the final numerical model can be written as:

$$\begin{bmatrix} \boldsymbol{K} & \boldsymbol{G} \\ \boldsymbol{G}^T & 0 \end{bmatrix} \begin{Bmatrix} \boldsymbol{d} \\ \boldsymbol{\lambda} \end{Bmatrix} = \begin{Bmatrix} \boldsymbol{f} \\ \boldsymbol{q} \end{Bmatrix} \quad (21)$$

such that

$$\boldsymbol{G} = \int_{\Gamma_u} \mathbf{\Psi}^T \mathbf{N} \mathbf{d}\Gamma_u \quad (22)$$

$$\boldsymbol{q} = \int_{\Gamma_u} \boldsymbol{N}^T \bar{\mathbf{u}} \mathbf{d}\Gamma_u \quad (23)$$

In (22) and (23), $\boldsymbol{N}$ denotes the standard finite element shape functions whereas $\Psi$ represents the MLS shape functions.

*D. The Level Set Method (LSM)*

The LSM has been used to keep track of the discontinuities produced by inclusions and cracks. This method defines the discontinuities by a zero value of a function called the level set function [16], [19], whose value is positive on one side of the interface and negative on the other side. The LSM has been extensively used in the modeling of different types of discontinuities such as cracks and inclusions [20], [21].

*E. Evaluation of Stress Intensity Factors*

The present study employs the domain based interaction integral approach [19] for evaluating the mixed mode stress intensity factors. The interaction integral can be written as:

$$M^{(1,2)} = \int_A \left[\sigma_{ij}^{(1)} \frac{\partial u_i^{(2)}}{\partial x_1} + \sigma_{ij}^{(2)} \frac{\partial u_i^{(1)}}{\partial x_1} - W^{(1,2)} \delta_{ij}\right] \frac{\partial q}{\partial x_j} dA \quad (24)$$

where, $'q'$ is a smooth weight function with a value of $'0'$ along the contour and $'1'$ at the crack tip. The state $'1'$ represents the actual state of the cracked body, whereas as state $'2'$ denotes the

auxiliary state. The mutual strain energy $W^{(1,2)}$ can be obtained as:

$$W^{(1,2)} = \frac{1}{2}\left(\sigma_{ij}^{(1)}\varepsilon_{ij}^{(2)} + \sigma_{ij}^{(2)}\varepsilon_{ij}^{(1)}\right) = \sigma_{ij}^{(1)}\varepsilon_{ij}^{(2)} = \sigma_{ij}^{(2)}\varepsilon_{ij}^{(1)} \quad (25)$$

where $'\varepsilon'$ represents the strains and $'\sigma'$ denotes the stresses. In terms of the stress intensity factors ($K_I$ and $K_{II}$), the interaction integral can be expressed as:

$$M^{(1,2)} = \frac{2}{E^*}\left(K_I^{(1)}K_I^{(2)} + K_{II}^{(1)}K_{II}^{(2)}\right) \quad (26)$$

where $E^* = \frac{E}{1-\mu^2}$ for plane strain and $E^* = E$ for plane stress. The mode-I stress intensity factors are obtained by choosing $K_I^{(2)} = 1$, $K_{II}^{(2)} = 0$, which gives $K_I^{(1)} = \frac{M^{(1,I)}E^*}{2}$. Similarly, the mode-II stress intensity factors can be obtained by selecting $K_I^{(2)} = 0$, $K_{II}^{(2)} = 1$, which gives $K_{II}^{(1)} = \frac{M^{(1,II)}E^*}{2}$.

### *F. Estimation of Crack Tip Plastic Zones*

The elastic stress field equations produce a stress singularity at the crack tip i.e. the stresses at the tip of the crack become infinite. But in actual practice, this is not possible because all the materials have a yield stress above which plastic deformation occurs and stress singularity cannot exist. There is a region around the crack tip where plastic deformation occurs, and this portion is called the crack tip plastic zone. The estimation of the size of the plastic zone around the crack tip is very important in fracture mechanics. The exact shape of the crack tip plastic zone can be obtained by applying the appropriate yield criterion. By applying the von Mises yield criteria, the shape of the crack tip plastic zone can be obtained for plane stress and plane strain conditions as:

$$r_p(\theta) = \frac{K_I^2}{4\pi\sigma_{ys}^2}\left[\frac{3}{2}sin^2\theta + (1-2\nu)^2(1+cos\theta)\right]; \quad (plane\ strain) \quad (27)$$

$$r_p(\theta) = \frac{K_I^2}{4\pi\sigma_{ys}^2}\left[1 + \frac{3}{2}sin^2\theta + cos\theta\right];\ (plane\ stress) \quad (28)$$

Similarly, the Tresca yield criterion gives:

$$r_p(\theta) = \frac{K_I^2}{2\pi\sigma_{ys}^2}cos^2\frac{\theta}{2}\left[1 - 2\nu + sin\frac{\theta}{2}\right]^2;(plane\ strain) \quad (29)$$

$$r_p(\theta) = \frac{K_I^2}{2\pi\sigma_{ys}^2}\left[cos\frac{\theta}{2}\left(1 + sin\frac{\theta}{2}\right)\right]^2;(plane\ stress) \quad (30)$$

## III. Numerical Results and Discussions

Now we investigate the effect of inclusions on the size and shape of plastic zones developed ahead of the crack tip by employing the EFGM. The effect of size and position of inclusions on the extent of the crack tip plastic zones is presented in this section. An edge cracked plate containing different inclusions at various positions is considered for simulation. The state of plane strain is considered for analysis. The length of the rectangular plate is 100 mm, whereas its height is $200\ mm$. The elastic moduli of the rectangular plate and the inclusions are $74\ GPa$ and $20\ GPa$, respectively. The Poisson's ratio has been taken as 0.3 for both. The plate is fixed at the bottom, whereas a static tensile load of $100\ N/mm$ is applied at the top edge, as shown in Fig. 1.

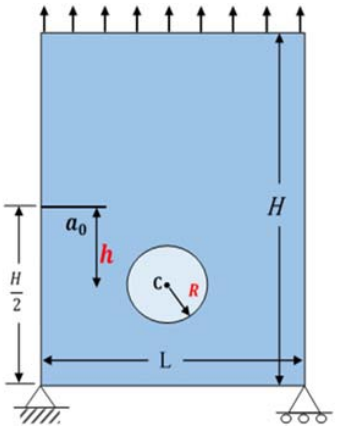


Fig. 1 Rectangular plate with an edge crack and inclusion

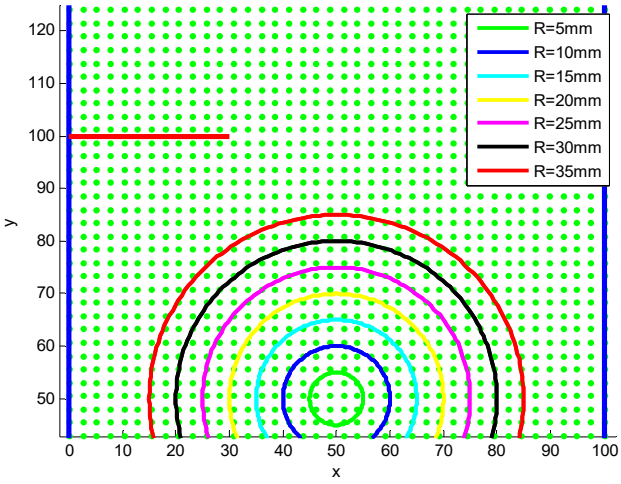


Fig. 2 Domain representation for different radii of inclusions in EFGM

### *A. Size of Inclusion*

The effect of the size of inclusions on the extent of crack tip plastic zones in presented here. The domain representation of an edge cracked plate containing different inclusions is shown in Fig. 2. The EFGM models the discontinuities produced by cracks and inclusions independent of the nodal distribution. The variations of stress intensity factors with load for different inclusions are shown in Fig. 3. The crack tip plastic zones for different sizes of inclusions, obtained by applying the von Mises and the Tresca yield criteria under plane stress conditions are shown in Figs. 4 and 5, respectively. The crack tip plastic zones for plane strain conditions are shown in Figs. 6 and 7. As expected, the size of plane strain crack tip plastic zones is much smaller than those of plane stress plastic zones.

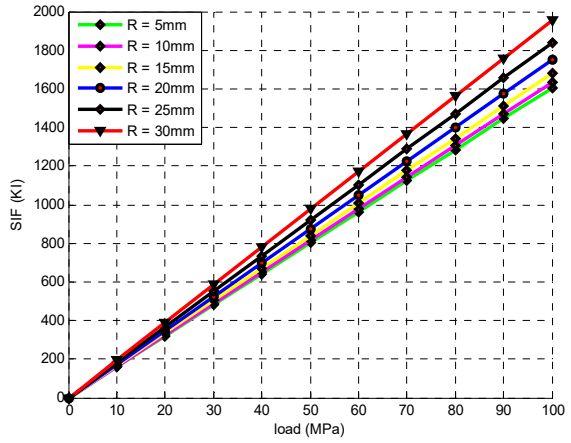


Fig. 3 Variation of stress intensity factors with load for different radii of inclusions

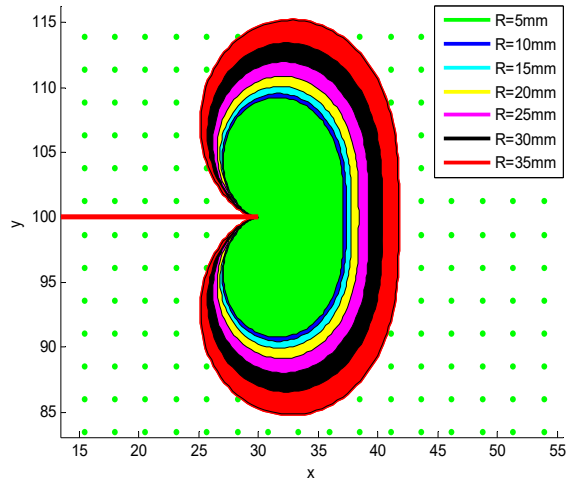


Fig. 4 Crack tip plastic zones for different radii of inclusions for plane stress conditions by von Mises Theory

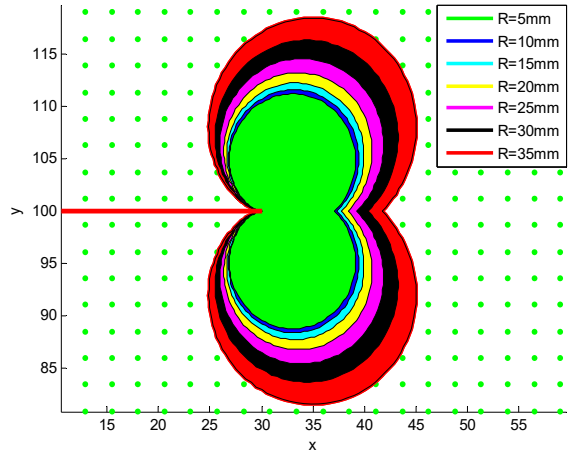


Fig. 5 Crack tip plastic zones for different radii of inclusions for plane stress conditions by von Mises Theory

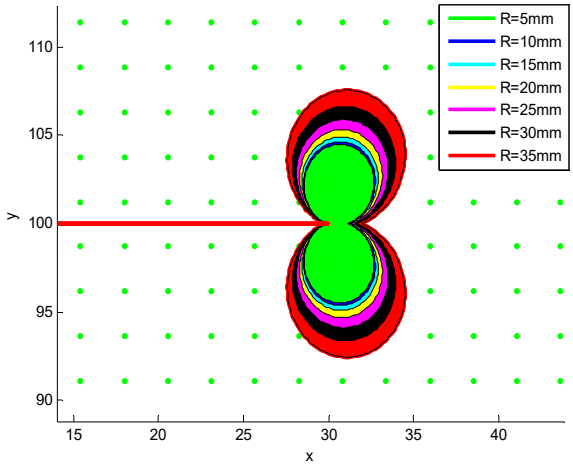


Fig. 6 Crack tip plastic zones for different radii of inclusions for plane strain conditions by von Mises Theory

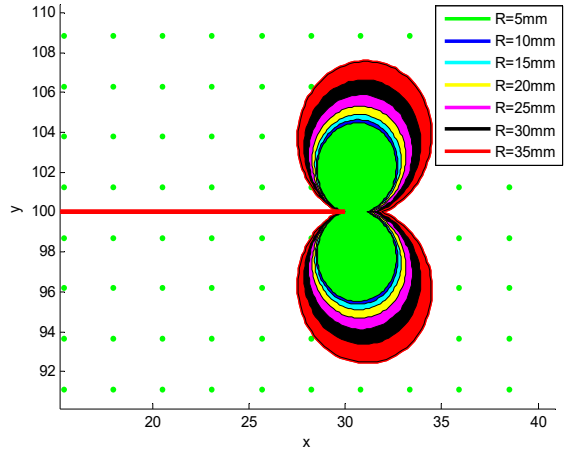


Fig. 7 Crack tip plastic zones for different radii of inclusions for plane strain conditions by Tresca Theory

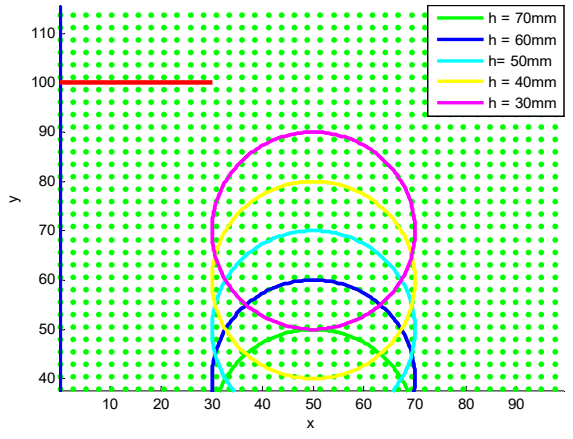


Fig. 8 Domain representation for positions of inclusions by EFGM

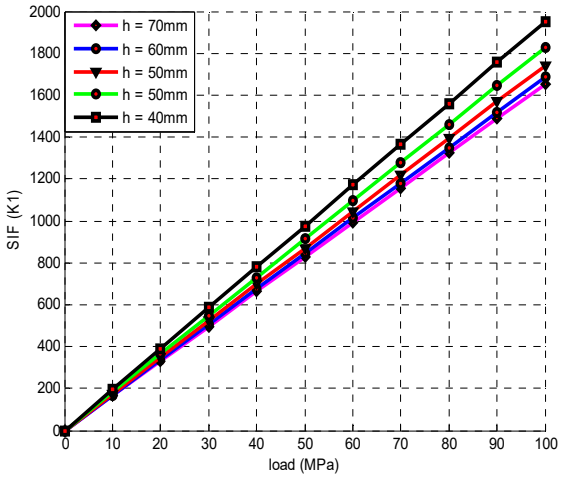


Fig. 9 Variation of stress intensity factors with load for different positions of inclusions

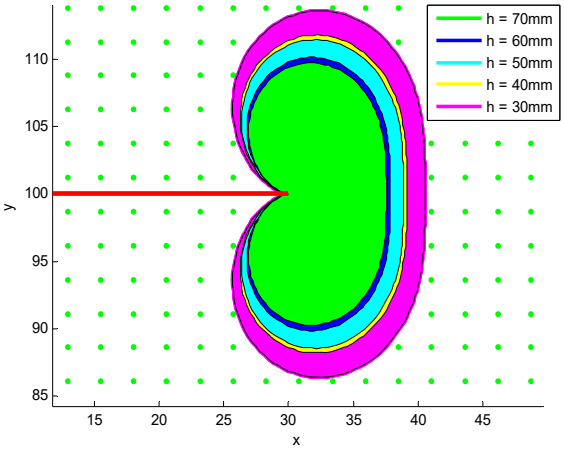


Fig. 10 Crack tip plastic zones for different positions of inclusions for plane stress conditions by von Mises Theory

### *B. Position of Inclusion*

The effect of the position of inclusions on crack tip plastic zones is presented here. The domain representation of an edge cracked plate containing inclusions at different positions is shown in Fig. 8. The variations of stress intensity factors with load are shown in Fig. 9. The crack tip plastic zones obtained by applying the von Mises and the Tresca yield criteria under plane stress conditions are shown in Figs. 10 and 11, respectively. The crack tip plastic zones for plane strain conditions are shown in Figs. 12 and 13. As expected, the size of plane strain crack tip plastic zones is much smaller than those of plane stress plastic zones.

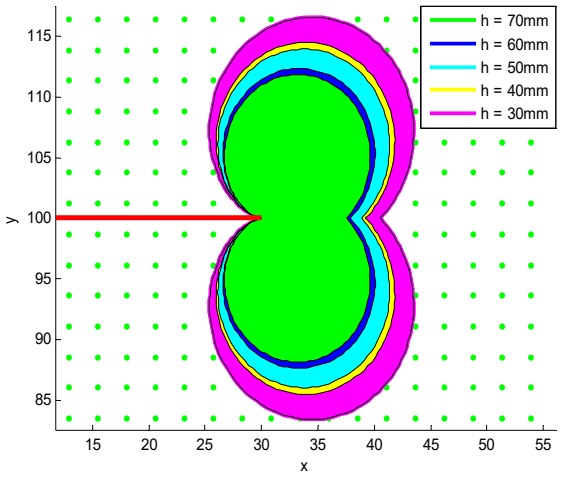


Fig. 11 Crack tip plastic zones for different positions of inclusions for plane stress conditions by Tresca Theory

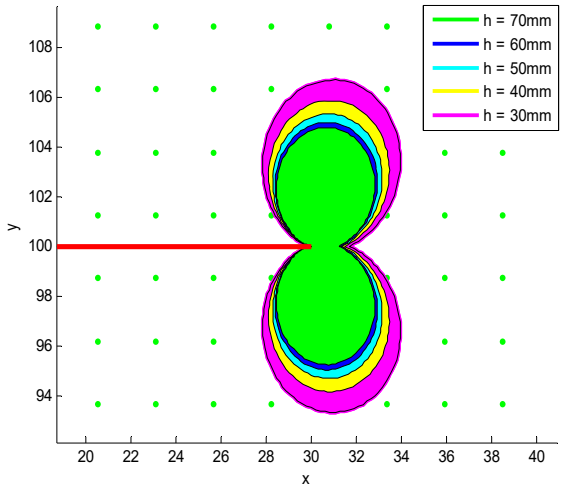


Fig. 12 Crack tip plastic zones for different positions of inclusions for plane strain conditions by von Mises Theory

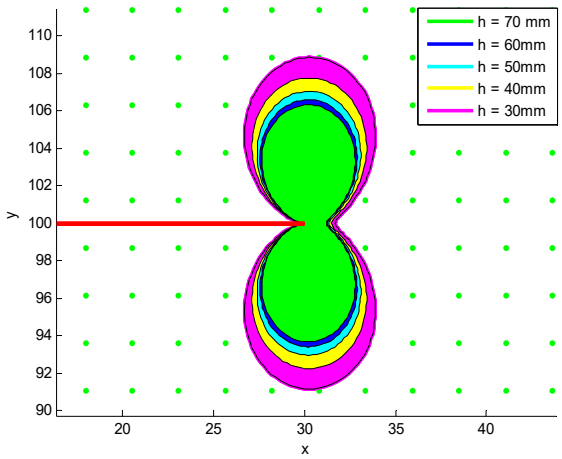


Fig. 13 Crack tip plastic zones for different positions of inclusions for plane strain conditions by Tresca Theory

## IV. Conclusions

The EFGM has been used to investigate the effect of inclusions on the size and shape of shape of the plastic zones developed ahead of the crack tip. EFGM provides a better numerical tool for modeling the discontinuities produced by cracks and inclusions because the modeling of discontinuities is independent of the mesh. Thus, the problems of conformal meshing, mesh refinement and re-meshing do not arise in EFGM. The presence of weak inclusions increases the size of the crack tip plastic zones. The extent of the crack tip plastic zone increases with the increase in the size of inclusions. The position of inclusions also affects the size of the plastic zones. The extent of the plastic zones increases as the inclusion approaches the crack.

## References

[1] Cheung, S. and Luxmoore A. R. (2003) A finite element analysis of stable crack growth in an aluminium alloy. Eng. Fract. Mech., 70, 1153–1169.
[2] Singh, I. V., Mishra, B. K., Bhattacharya, S. and Patil, R. U. (2012) The numerical simulation of fatigue crack growth using extended finite element method. Int. J. Fatigue, 36, 109–119.
[3] Jameel, A. and Harmain, G. A. (2016) Modeling and numerical simulation of fatigue crack growth in cracked specimens containing material discontinuities. Strength of Materials, 48, 294–306.
[4] Yan, A. M. and Nguyen-Dang, H. (1995) Multiple-cracked fatigue crack growth by BEM. Comput. Mech., 16, 273–280.
[5] Pant, M., Singh, I. V. and Mishra, B. K. (2010) Numerical simulation of thermo-elastic fracture problems using element free Galerkin method. Int. J. Mech. Sci., 52, 1745–1755.
[6] Belytschko, T., Lu, Y. Y. and Gu, L. (1995) Crack propagation by element-free Galerkin methods. Eng. Fract. Mech., 51, 295–315.
[7] Marc Duflot and Hung Nguyen-Dang. (2004) A meshless method with enriched weight functions for fatigue crack growth. Int. J. Numer. Methods Eng., 59, 1945–1961.
[8] Marc Duflot and Hung Nguyen-Dang. (2004) Fatigue crack growth analysis by an enriched meshless method. J. Comput. Appl. Math., 168, 155–164.
[9] Lancaster, P. and Salkauskas, K. (1981) Surfaces generated by moving least square methods. Math. Comput., 37, 141–158.
[10] Belytschko, T., Gu, L. and Lu, Y. Y. (1994) Fracture and crack growth by element-free Galerkin methods. Modell. Simul. Mater. Sci. Eng., 2, 519–534.
[11] Lu, Y. Y., Belytschko, T. and Gu, L. (1994) A new implementation of the element free Galerkin method. Comput. Methods Appl. Mech. Eng., 113, 397–414.
[12] Krongauz, Y. and Belytschko, T. (1996) Enforcement of essential boundary conditions in meshless approximations using finite elements. Comput. Methods Appl. Mech. Eng., 131, 133–145.
[13] Mukherjee, Y. X. and Mukherjee S. (1997) On boundary conditions in the element-free Galerkin method. Comput. Mech., 19, 264-270.
[14] Xu, Y. and Saigal, S. (1998) An element free Galerkin formulation for stable crack growth in an elastic solid. Comput. Methods Appl. Mech. Eng., 154, 331–343.
[15] Li, G. Y. and Belytschko, T. (2001) Element-free Galerkin method for contact problems in metal forming analysis. Eng. Comput., 18 (1), 62–78.
[16] Yanjin, G., Xin, W., Zhao, G. and Ping, L. (2009) A nonlinear numerical analysis for metal forming process using the rigid-(visco) plastic element free Galerkin method. Int. J. Adv. Manuf. Technol., 42, 83–92.
[17] Jameel, A. and Singh T. (2014) Modeling and Simulation of Large Deformation Bi-material Problems Using EFGM. Inroads, 3 (1), 48–53.
[18] Sukumar, N., Moran, B., Black, T. and Belytschko, T. (1997) An element-free Galerkin method for the three-dimensional fracture mechanics. Comput. Mech., 20, 170–175.
[19] Jameel, A. and Harmain, G. A. (2015) Fatigue crack growth in presence of material discontinuities by EFGM. Int. J. Fatigue, 81, 105-116.
[20] Belytschko, T., Krongauz, Y., Organ, D., Fleming, M. and Krysl, P. (1996) Meshless methods: An overview and recent developments. Comput. Methods Appl. Mech. Eng., 139, 3-47.
[21] Yazid, A., Abdelkader N. and Abdelmadjid H. (2009) A state-of-the-art review of the X-FEM for computational fracture mechanics. Appl. Math. Modelling., 33, 4269–4282.